

Metallic Icosahedron Phase of Sodium at Terapascal Pressures

Yinwei Li,^{1,2} Yanchao Wang,² Chris J. Pickard,³ Richard J. Needs,⁴ Yi Wang,⁵ and Yanming Ma^{2,*}

¹*School of Physics and Electronic Engineering, Jiangsu Normal University, Xuzhou 221116, China*

²*State Key Laboratory of Superhard Materials, Jilin University, Changchun 130012, China*

³*Department of Physics and Astronomy, University College London, Gower Street, London WC1E 6BT, United Kingdom*

⁴*Theory of Condensed Matter Group, Cavendish Laboratory, J J Thomson Avenue, Cambridge CB3 0HE, United Kingdom*

⁵*Natural Science Research Center, Academy of Fundamental and Interdisciplinary Sciences, Harbin Institute of Technology, Harbin 150080, China*

(Received 5 December 2014; published 23 March 2015)

Alkali metals exhibit unexpected structures and electronic behavior at high pressures. Compression of metallic sodium (Na) to 200 GPa leads to the stability of a wide-band-gap insulator with the double hexagonal *hP4* structure. Post-*hP4* structures remain unexplored, but they are important for addressing the question of the pressure at which Na reverts to a metal. Here, we report the reentrant metallicity of Na at the very high pressure of 15.5 terapascal (TPa), predicted using first-principles structure searching simulations. Na is therefore insulating over the large pressure range of 0.2–15.5 TPa. Unusually, Na adopts an *oP8* structure at pressures of 117–125 GPa and the same *oP8* structure at 1.75–15.5 TPa. The metallization of Na occurs on the formation of a stable and striking body-centered cubic *cI24* electrone structure consisting of Na₁₂ icosahedra, each housing at its center about one electron that is not associated with any Na ions.

DOI: 10.1103/PhysRevLett.114.125501

PACS numbers: 61.50.Ks, 61.50.Ah, 62.50.-p, 71.20.-b

Alkali metals have long been known to possess simple electronic structures at ambient pressure that are well explained by a nearly free-electron model. However, the simple low-pressure structures of alkali metals do not remain simple upon compression. Rich and complex phases and remarkable physical phenomena have been observed, such as greatly increased electrical resistivity [1], enhanced superconductivity [2,3], unusually low melting temperatures [4,5] and metal-insulator–semiconductor transitions [6,7].

The metal-insulator transitions in Na and lithium (Li) [6,7] are among the most fascinating observations at high pressure. Neaton and Ashcroft predicted that upon compression Li [8] and Na [9] might transform into atomically paired structures. If a paired structure was to be adopted, both Na and Li would have the potential to be semiconducting. These predictions have stimulated numerous studies of the high-pressure structures of Li and Na (e.g., Refs. [6,7,10–14]).

The metal-insulator transition in Na was established by a joint theoretical and experimental effort [7] and confirmed by further experiments [15]. Na is predicted and observed to transform into an optically transparent phase at above 200 GPa [7]. This phase was predicted and experimentally confirmed to have a double hexagonal *hP4* structure [7], with a remarkably large band gap reaching 6.5 eV at 600 GPa. A metal-semiconductor transition was observed in Li at 80 GPa. The semiconducting structure of dense Li remained unsolved despite considerable attention (e.g., Refs. [11–14]). Blind crystal structure prediction calculations [12] on dense Li predicted a complex semiconducting *oC40* structure. Independent experimental and theoretical studies also found that semiconducting Li adopts the *oC40* structure [16].

Analysis of the charge density [7,11,12] shows that the emergence of an insulating state in dense Na/Li is, however, not attributable to atomic pairing, but rather to strong localization of valence electrons within lattice voids. Notably, the insulating phases of Na and Li can be regarded as prototypical examples of electrides [17], in which the ionic cores play the role of cations, and interstitial electrons form the anions [7,11,12]. Stable electride structures have also been predicted in other elements at high pressures, e.g., Al [18], Mg [19], Ca [20], and K [21]. The formation of an electride in Na at high pressures is favorable because it reduces the kinetic energy of the higher-energy electrons. These electronic orbitals are forced to oscillate rapidly close to the atomic cores due to Pauli repulsion, but if they move away from the cores the oscillations and, hence, the kinetic energy can be reduced [17,18]. The electrides have open structures if one considers only the ions, but when the interstitial electrons are considered as anions the structures make good chemical sense as ionic solids.

Pressure-induced metal-insulator transitions have been predicted in other materials at TPa pressures. For example, it was suggested that Mg, a good metal at normal pressures, would transform from a metal to a semimetal at 24 TPa [22], and Ni was predicted to transform to an insulator at 34 TPa [23]. The metal-insulator transition in Ni is driven by the complete $4s \rightarrow 3d$ charge transfer under pressure, which is different from the electron localization found in Li and Na.

Metallization is presumed to be the ultimate fate of all materials under sufficiently strong compression [24]. The insulating phase of Ni has been predicted to revert to metallic behavior at 51 TPa [23]. Recent electrical resistance measurements have revealed that semiconducting Li

reverts to a “poor metal” above 120 GPa [10]. The question of the pressure at which Na will also revert to a metal remains unanswered. Determining the ground-state structures of Na at high pressures provides the key to whether insulating or metallic behavior is observed. At room temperature, Na undergoes pressure-induced phase transitions with an established sequence of $bcc \rightarrow fcc$ (65 GPa) [25] $\rightarrow cI16$ (103 GPa) [26–28] $\rightarrow oP8$ (117 GPa) [26] $\rightarrow tI19$ (125 GPa) [26] $\rightarrow hP4$ (200 GPa) [7]. The $hP4$ structure is the highest-pressure phase of Na known so far.

In this Letter, we report the reentrant metallicity of Na at a surprisingly high pressure of 15.5 TPa, predicted via extensive structure searching in conjunction with first-principles calculations. We predict that Na will show insulating behavior over a remarkably large pressure range of 0.2–15.5 TPa and will exhibit a phase transition to a second insulating orthorhombic $oP8$ structure at 1.75 TPa. Metallization of Na appears with the formation of a striking body-centered cubic (bcc) $cI24$ structure whose lattice sites are populated by Na_{12} icosahedra, each containing about one electron that is not associated with any Na ions.

Our structure searching calculations with simulation cells containing up to 24 atoms were performed in a wide pressure range (0.4–20 TPa). We used the efficient CALYPSO [29,30] and AIRSS [31,32] methods, which have both been successfully applied to investigating structures of materials at high pressures [12,31,33–42]. TPa pressures can now be achieved with dynamic ramped compression. In particular, diamond has been studied experimentally up to 5 TPa [43]. The density functional theory [44] calculations were performed using the CASTEP plane-wave code [45] with the Perdew-Burke-Ernzerhof [46] (PBE) generalized gradient approximation functional. We performed calculations with both norm-conserving and ultrasoft Na pseudopotentials, in which only the $1s$ energy level was treated as core. An ultrasoft pseudopotential was used for the structure searches, with a plane-wave cutoff energy of 910 eV and a Brillouin-zone integration grid spacing of $2\pi \times 0.05 \text{ \AA}^{-1}$. The structures obtained were reoptimized at a higher level of accuracy for both the norm-conserving and ultrasoft pseudopotentials. Here, we present only norm-conserving results since the two pseudopotentials led to consistent conclusions. A cutoff energy of 1633 eV and a k -point grid spacing of $2\pi \times 0.03 \text{ \AA}^{-1}$ were used in the calculations with norm-conserving pseudopotentials. The phonon dispersion curves were computed by a finite displacement method as implemented in the CASTEP code.

Our structure searches readily reproduced the known double hexagonal $hP4$ structure (space group $P6_3/mmc$, 4 atoms/unit cell) above 400 GPa, and we found no better structure below 1.5 TPa. Surprisingly, above 2 TPa, we found the reappearance of the orthorhombic $oP8$ structure [space group $Pnma$, 8 atoms/unit cell, Fig. 1(a)] which is also observed at low pressures of 117–125 GPa [26].

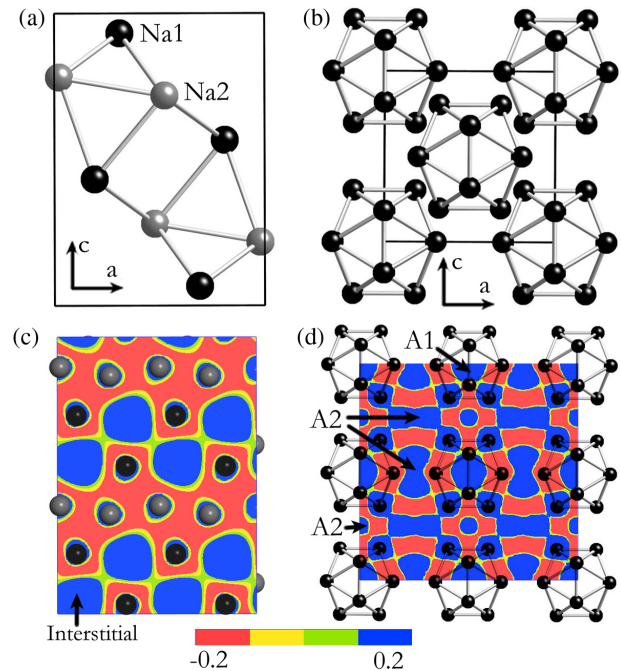


FIG. 1 (color online). Crystal structures of $oP8$ (a) and $cI24$ (b) and their electron density difference maps [(c) and (d)] at ultrahigh pressures. The lattice parameters of $oP8$ -Na at 2 TPa are $a = 2.88 \text{ \AA}$, $b = 2.12 \text{ \AA}$, and $c = 4.0 \text{ \AA}$ with two inequivalent Na1 and Na2 atoms at $4c$ positions of (0.809, 0.75, 0.567) and (0.523, 0.25, 0.719), respectively. For $cI24$ -Na at 16 TPa, $a = 3.12 \text{ \AA}$ with Na atoms at $24g$ positions (0, 0.302, 0.183). Electron density differences are plotted within the (010) plane of $oP8$ -Na (c) at 2 TPa and $cI24$ -Na (d) at 16 TPa, respectively. A1 and A2 in (d) represent electron attractors located at the centers of the Na_{12} icosahedra and octahedral voids formed by the six neighboring Na_{12} icosahedra, respectively.

Strikingly, we predict a hitherto unexpected highly symmetric bcc structure at 20 TPa [space group $Im-3$, 24 atoms/unit cell, denoted $cI24$ hereafter, see Fig. 1(b)]. The $cI24$ structure consists of Na_{12} cages, each of which contains 12 Na atoms forming an icosahedron. The shortest intra- and intericosahedral Na-Na distances at 16 TPa are calculated to be 1.138 and 1.168 \AA , respectively, indicating fairly strong core-core overlap (the ionic radius of Na^+ is 1.02 \AA). An analysis of electron density differences [Fig. 1(d)] reveals that the $cI24$ phase is also an electrider with two distinct electron attractors located at the centers of the Na_{12} icosahedra (A1) and the octahedral voids (A2). However, unlike the nearly spherical isosurface of the interstitial electrons in the $hP4$ and $oP8$ structures, dumbbell-like electron localization is found in the octahedral voids.

The enthalpies of the $oP8$ (relative to $hP4$) and $cI24$ (relative to $oP8$) phases are plotted as functions of pressure in Figs. 2(a) and 2(b), respectively. The inset to Fig. 2(a) shows that $hP4$ -Na transforms to the $oP8$ structure at 1.75 TPa with a continuous volume change, indicating a

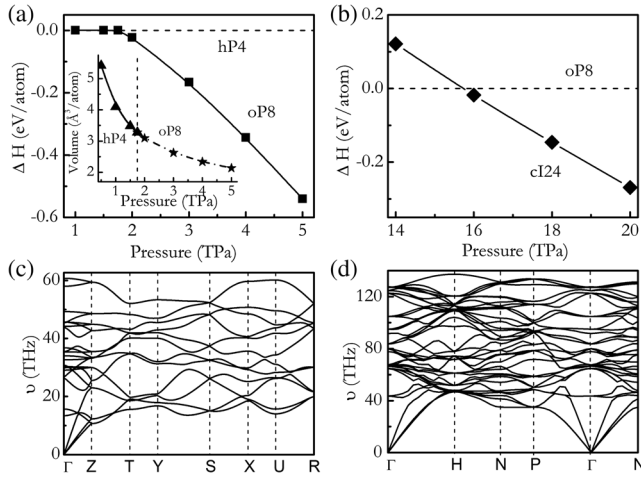


FIG. 2. Enthalpy differences relative to *hP4* (a) and *oP8* (b) of Na as a function of pressure. The inset in (a) shows the pressure dependence of the volumes of the *hP4* and *oP8* phases. The predicted sequence of phase transitions at zero temperature in the pressure range of 0–20 TPa is provided in Fig. S1 of the Supplemental Material [47]. The volume appears to change continuously across the phase transition. [(c) and (d)] Calculated phonon dispersion relations of *oP8*-Na at 2 TPa and *cI24*-Na at 16 TPa, respectively.

second-order phase transition. The *oP8* phase remains stable up to 15.5 TPa, above which the *cI24* phase becomes the most stable. Phonon calculations for *oP8* and *cI24*-Na in their corresponding stable pressure ranges show no imaginary frequencies, demonstrating the dynamical stability of the structures [Figs. 2(c), 2(d)]. The maximum frequency in the TPa pressure regime reaches 137 THz at 16 TPa, which is very high and implies a large nuclear zero-point (ZP) energy. The estimated ZP energies within the quasiharmonic approximation are indeed extremely large: 0.577 and 0.585 eV/atom for *cI24* and *oP8* phases at 20 TPa, respectively. However, the difference in ZP energies of only 8 meV/atom is too small to modify the phase diagram of Na at TPa pressures. Furthermore, we have calculated the Gibbs free energies of the *cI24* and *oP8* phases at 20 TPa within the quasiharmonic approximation at finite temperatures to account for vibrational contributions. The resultant difference in free energy between *cI24* and *oP8* at 1000 K is only 3 meV/atom larger than that at 0 K [Fig. 2(b)], which gives a negligible change in the *oP8*-*cI24* transition pressure.

We calculated the phonon dispersion curves of *hP4*-Na at various pressures in order to understand the origin of the reemergence of the *oP8* phase and the second-order nature of the *hP4*-*oP8* transition. We found that a transverse acoustic (TA) phonon mode at the zone boundary *M* (0,0.5,0) point softens with increasing pressure [Fig. 3(a)], and its frequency goes to zero at 1.72 TPa [Fig. 3(b)]. A frozen-phonon calculation was performed by distorting the *hP4* structure according to the atomic

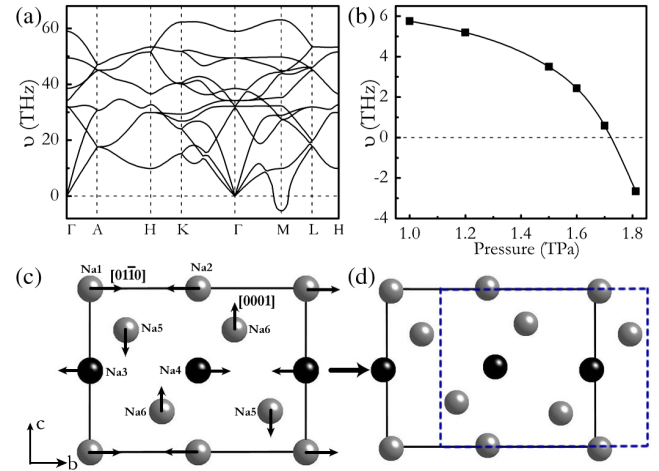


FIG. 3 (color online). Phonon dispersion curves of *hP4*-Na at 2 TPa (a) and the phonon frequencies of the softened TA phonon mode at *M* (0, 0.5, 0) as a function of pressure (b). (c) Atomic vibrations of the soft TA mode at the *M* point viewed along the *a* axis in a $1 \times 2 \times 1$ supercell of the *hP4* structure. Here, the Na1 (Na2) and Na4 (Na3) atoms vibrate parallel (antiparallel) to the $[01\bar{1}0]$ direction, while the Na5 (Na6) atoms vibrate antiparallel (parallel) to the $[0001]$ direction. The gray and black balls indicate atoms in different planes. Arrows indicate vibrational direction of different Na atoms as labeled and are plotted from the eigenvector of the TA soft mode at the *M* point. The blue dashed cell in (d) indicates the *oP8* structure resulting from the distortion.

vibrations for the TA mode at the *M* point as depicted in Fig. 3(c), and structural optimizations were subsequently carried out. The resultant energetically stable structure is indeed the orthorhombic *oP8* phase, as indicated by the dashed cell in Fig. 3(d). It is clear that the *hP4*-*oP8* transition is driven by the soft TA mode. This result is consistent with the second-order *hP4*-*oP8* transition characterized by a continuous volume change [inset in Fig. 2(a)]. Soft-phonon-driven *hP4*-*oP8* transformations have also been reported in MnAs, CrTe, MnTe, MgTe, CrSb, and CaH₂ [48–50].

The electronic band structures and band gaps of *hP4*, *oP8*, and *cI24*-Na were calculated at selected pressures using the HSE06 functional [51,52], which is known to give better band gaps than the standard PBE functional. The band gap of *hP4*-Na increases with pressure and reaches 9.5 eV at the transition to the *oP8* phase at 1.75 TPa. At the transition, *oP8*-Na is also a wide-band-gap insulator with an even larger gap of 9.7 eV [Fig. 4(a)]. The gap of *oP8*-Na decreases with pressure down to 1.6 eV at 15.5 TPa. The *oP8* structure is compressed by a factor of 3 from 125 GPa (volume = 77.9 \AA^3 per unit cell) to 1.75 TPa (volume = 25.9 \AA^3 per unit cell). As a result of this strong compression, the *oP8* structure at TPa pressures forms an electride with valence electrons trapped at the interstitial sites [Fig. 1(c)]. The electronic structure is fundamentally different from that of the nearly free-electron behavior of *oP8* at a much lower pressure of

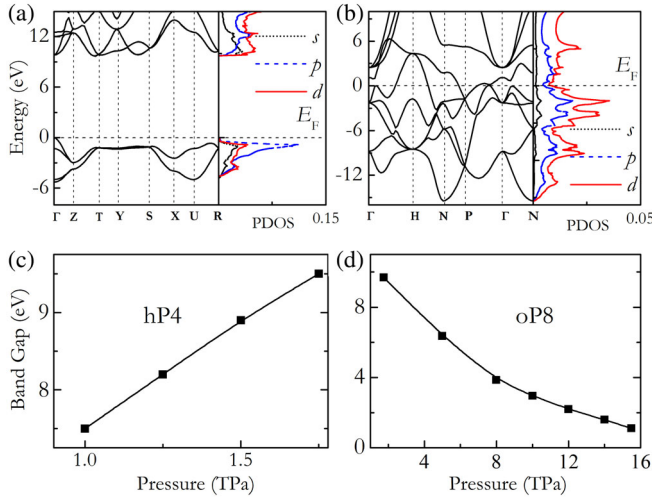


FIG. 4 (color online). Electronic band structure and projected density of states of *oP8*-Na at 1.75 TPa (PDOS, in units of eV^{-1} per atom) (a) and *cI24*-Na at 16 TPa (b). The horizontal dotted lines indicate the Fermi level. [(c) and (d)] Variation of band gaps with pressure for *hP4* and *oP8*-Na, respectively, using the HSE06 functional.

125 GPa (Supplemental Material Fig. S2 [47]). As a result, the *oP8* phase is insulating at TPa pressures but is metallic at pressure below 125 GPa [26,47].

After the transition to the *cI24* phase, the localized electrons in the octahedral voids are partially squeezed out due to the decreasing interstitial space, forming a series of conducting channels between *A2* attractors and Na cations, as shown in Fig. 1(d). Notably, the band structure of *cI24*-Na at 16 TPa shows highly dispersive bands crossing the Fermi level [Fig. 4(b)] and the return to metallicity.

The enthalpy $H = U + PV$ governs the phase stability at 0 K. Under sufficiently strong compression, the hard core repulsion between atoms becomes very important, and it favors close-packed structures such as (*bcc*, *fcc* or *hcp*) [53], which have small volumes V . However, the *cI24* structure that Na adopts at TPa pressure is far from simple and is constructed from Na_{12} icosahedral cages, further challenging the established picture of simple packing at high densities. Indeed, our optimized hypothetical *bcc* structure with Na atoms occupying the lattice sites at 20 TPa gives a volume of $1.175 \text{ \AA}^3/\text{atom}$, which has a lower density than *cI24*-Na ($1.148 \text{ \AA}^3/\text{atom}$) whose *bcc* lattice sites are occupied by Na_{12} icosahedral cages. Integration of the electron density at 16 TPa shows that the charge on each Na atom is depleted by about ~ 0.35 electrons, while the cage-center *A1* and interstitial *A2* sites [Fig. 1(d)] have excess electronic charges of about ~ 1.2 and ~ 1.0 electrons, respectively. As a whole, 9 of the 12 valence electrons remain within each Na_{12} cage (including the localized central electrons), while 3 electrons localize in the octahedral voids. The 9-electron configuration might allow a Na_{12} cage to be termed a superalkali atom.

Electronically, a Na_{12} cage resembles a potassium atom with an electronic configuration of $3s^2 3p^6 4s^1$.

Cagelike structures are seldom seen at high pressures since they do not usually favor dense packing. Known cage structures are typically found in elements in which it is easy to form covalent bonds. Examples occur in various allotropes of B ($\alpha\text{-B}_{12}$ [54] and $\gamma\text{-B}_{28}$ [55]) and C (C_{60} and C_{70}) [56] and Si/Ge cages in clathrates (e.g., in $\text{Ba}_8\text{Si}_{46}$ [57]). In recent work, we also found a N_{10} cage structure in polymeric nitrogen [58] and a H_{24} cage in hydrogen-rich CaH_6 [37]. Here, the formation of Na_{12} icosahedra is rather surprising since Na is unable to stabilize covalent bonds. The Na_{12} cage is geometrically similar to a B_{12} cage, which is the fundamental building block of various boron allotropes [54,55]. B is electron deficient and forms multicenter covalent bonds. Three-center covalent bonds within the icosahedra and two- or three-center covalent bonds between the icosahedra in various structures of elemental B satisfy the octet rule and generate insulating states. Here, there is no covalent bonding within the Na_{12} cages, and it is actually a well-packed ionic structure. The electrons at the center of the cage contribute to the stability of the Na_{12} cages and play a role similar to that of Ba atoms in the $\text{Ba}_8\text{Si}_{46}$ clathrate structure [57].

We find that *cI24*-Na is structurally similar to the *bcc* form of the Al_{12}W alloy [59], in which Al_{12} also forms an icosahedral cage with a W atom localized at its center, and the W-encaged Al_{12} icosahedrons occupy *bcc* lattice sites. One Al_{12}W unit resembles a Na_{12} icosahedron, and the encaged electron plays the role of the pseudoions in W. In contrast to the single dumbbell-like electron attractor found in the octahedral voids of *cI24*-Na, the voids in Al_{12}W contain four distinct dumbbell-like electron attractors (Supplemental Material Fig. S5 [47]).

Na is insulating over the large pressure range of 0.2–15.5 TPa. The pressure interval of 15.3 TPa (98.7% of the pressure range 0–15.5 TPa) is comparable to the 17 TPa (33.3% of the whole pressure range) pressure interval predicted for the insulating phase of Ni [23]. The pressure for reentrant metallicity in Na (15.5 TPa) is much higher than that in Li (120 GPa), which may be associated with the entirely different mechanism for insulating behavior. In the *hP4* and *oP8* structures of Na, the valence electrons localize strongly within the lattice interstices and maintain a nearly spherical shape [Fig. 1(c)] up to 15.5 TPa. However, semiconducting Li has a complex *oC40* structure with interstitial regions of different shapes in which electrons are localized at a rather low pressure of 80 GPa. These localized electrons are connected to each other and form conducting channels at 120 GPa (Supplemental Material [47]).

Y. L., Y. W., and Y. M. acknowledge funding from the China 973 Program under Grant No. 2011CB808200 and the National Natural Science Foundation of China under Grants No. 11274136, No. 11025418, and No. 91022029.

Y. L. also acknowledges funding from the National Natural Science Foundation of China under Grants No. 11204111 and No. 11404148, the Natural Science Foundation of Jiangsu province under Grant No. BK20130223, and the PAPD of Jiangsu Higher Education Institutions. C. J. P. and R. J. N. acknowledge funding from the Engineering and Physical Sciences Research Council of the U.K.

*mym@jlu.edu.cn

- [1] V. E. Fortov, V. V. Yakushev, K. L. Kagan, I. V. Lomonosov, V. I. Postnov, and T. I. Yakusheva, *JETP Lett.* **70**, 628 (1999).
- [2] J. Wittig, *Phys. Rev. Lett.* **24**, 812 (1970).
- [3] V. V. Struzhkin, M. I. Eremets, W. Gan, H. K. Mao, and R. J. Hemley, *Science* **298**, 1213 (2002).
- [4] C.-S. Zha and R. Boehler, *Phys. Rev. B* **31**, 3199 (1985).
- [5] E. Gregoryanz, O. Degtyareva, M. Somayazulu, R. J. Hemley, and H.-k. Mao, *Phys. Rev. Lett.* **94**, 185502 (2005).
- [6] T. Matsuoka and K. Shimizu, *Nature (London)* **458**, 186 (2009).
- [7] Y. Ma, M. Eremets, A. R. Oganov, Y. Xie, I. Trojan, S. Medvedev, A. O. Lyakhov, M. Valle, and V. Prakapenka, *Nature (London)* **458**, 182 (2009).
- [8] J. B. Neaton and N. W. Ashcroft, *Nature (London)* **400**, 141 (1999).
- [9] J. B. Neaton and N. W. Ashcroft, *Phys. Rev. Lett.* **86**, 2830 (2001).
- [10] T. Matsuoka, M. Sakata, Y. Nakamoto, K. Takahama, K. Ichimaru, K. Mukai, K. Ohta, N. Hirao, Y. Ohishi, and K. Shimizu, *Phys. Rev. B* **89**, 144103 (2014).
- [11] M. Marqués, M. I. McMahon, E. Gregoryanz, M. Hanfland, C. L. Guillaume, C. J. Pickard, G. J. Ackland, and R. J. Nelmes, *Phys. Rev. Lett.* **106**, 095502 (2011).
- [12] J. Lv, Y. Wang, L. Zhu, and Y. Ma, *Phys. Rev. Lett.* **106**, 015503 (2011).
- [13] Y. Yao, J. S. Tse, and D. D. Klug, *Phys. Rev. Lett.* **102**, 115503 (2009).
- [14] C. J. Pickard and R. J. Needs, *Phys. Rev. Lett.* **102**, 146401 (2009).
- [15] M. Marqués, M. Santoro, C. L. Guillaume, F. A. Gorelli, J. Contreras-García, R. T. Howie, A. F. Goncharov, and E. Gregoryanz, *Phys. Rev. B* **83**, 184106 (2011).
- [16] C. L. Guillaume, E. Gregoryanz, O. Degtyareva, M. I. McMahon, M. Hanfland, S. Evans, M. Guthrie, S. V. Sinogeikin, and H. K. Mao, *Nat. Phys.* **7**, 211 (2011).
- [17] M.-S. Miao and R. Hoffmann, *Acc. Chem. Res.* **47**, 1311 (2014).
- [18] C. J. Pickard and R. Needs, *Nat. Mater.* **9**, 624 (2010).
- [19] P. Li, G. Gao, Y. Wang, and Y. Ma, *J. Phys. Chem. C* **114**, 21745 (2010).
- [20] A. R. Oganov, Y. Ma, Y. Xu, I. Errea, A. Bergara, and A. O. Lyakhov, *Proc. Natl. Acad. Sci. U.S.A.* **107**, 7646 (2010).
- [21] C. J. Pickard and R. J. Needs, *Phys. Rev. Lett.* **107**, 087201 (2011).
- [22] J. A. Moriarty and A. K. McMahan, *Phys. Rev. Lett.* **48**, 809 (1982).
- [23] A. K. McMahan and R. C. Albers, *Phys. Rev. Lett.* **49**, 1198 (1982).
- [24] E. Wigner and H. Huntington, *J. Chem. Phys.* **3**, 764 (1935).
- [25] M. Hanfland, I. Loa, and K. Syassen, *Phys. Rev. B* **65**, 184109 (2002).
- [26] E. Gregoryanz, L. F. Lundegaard, M. I. McMahon, C. Guillaume, R. J. Nelmes, and M. Mezouar, *Science* **320**, 1054 (2008).
- [27] M. I. McMahon, E. Gregoryanz, L. F. Lundegaard, I. Loa, C. Guillaume, R. J. Nelmes, A. K. Kleppe, M. Amboage, H. Wilhelm, and A. P. Jephcoat, *Proc. Natl. Acad. Sci. U.S.A.* **104**, 17297 (2007).
- [28] M. Hanfland, K. Syassen, L. Loa, N. E. Christensen, and D. L. Novikov, *Poster at 2002 High Pressure Gordon Conference, 2002*.
- [29] Y. Wang, J. Lv, L. Zhu, and Y. Ma, *Phys. Rev. B* **82**, 094116 (2010).
- [30] Y. Wang, J. Lv, L. Zhu, and Y. Ma, *Comput. Phys. Commun.* **183**, 2063 (2012).
- [31] C. J. Pickard and R. J. Needs, *Phys. Rev. Lett.* **97**, 045504 (2006).
- [32] C. J. Pickard and R. J. Needs, *J. Phys. Condens. Matter* **23**, 053201 (2011).
- [33] Q. Li, D. Zhou, W. Zheng, Y. Ma, and C. Chen, *Phys. Rev. Lett.* **110**, 136403 (2013).
- [34] L. Zhu, Z. Wang, Y. Wang, G. Zou, H. Mao, and Y. Ma, *Proc. Natl. Acad. Sci. U.S.A.* **109**, 751 (2011).
- [35] L. Zhu, H. Wang, Y. Wang, J. Lv, Y. Ma, Q. Cui, Y. Ma, and G. Zou, *Phys. Rev. Lett.* **106**, 145501 (2011).
- [36] Y. Wang, H. Liu, J. Lv, L. Zhu, H. Wang, and Y. Ma, *Nat. Commun.* **2**, 563 (2011).
- [37] H. Wang, S. T. John, K. Tanaka, T. Iitaka, and Y. Ma, *Proc. Natl. Acad. Sci. U.S.A.* **109**, 6463 (2012).
- [38] C. J. Pickard and R. J. Needs, *J. Chem. Phys.* **127**, 244503 (2007).
- [39] C. J. Pickard and R. J. Needs, *Nat. Phys.* **3**, 473 (2007).
- [40] J. M. McMahon and D. M. Ceperley, *Phys. Rev. Lett.* **106**, 165302 (2011).
- [41] C. J. Pickard, M. Martínez-Canales, and R. J. Needs, *Phys. Rev. B* **85**, 214114 (2012).
- [42] J. Sun, M. Martínez-Canales, D. D. Klug, C. J. Pickard, and R. J. Needs, *Phys. Rev. Lett.* **108**, 045503 (2012).
- [43] R. Smith, J. Eggert, R. Jeanloz, T. Duffy, D. Braun, J. Patterson, R. Rudd, J. Biener, A. Lazicki, and A. Hamza, *Nature (London)* **511**, 330 (2014).
- [44] S. Baroni, P. Giannozzi, and A. Testa, *Phys. Rev. Lett.* **58**, 1861 (1987).
- [45] S. J. Clark, M. D. Segall, C. J. Pickard, P. J. Hasnip, M. I. Probert, K. Refson, and M. C. Payne, *Z. Kristallogr.* **220**, 567 (2005).
- [46] J. P. Perdew, K. Burke, and M. Ernzerhof, *Phys. Rev. Lett.* **77**, 3865 (1996).
- [47] See the Supplemental Material at <http://link.aps.org/supplemental/10.1103/PhysRevLett.114.125501> for phase sequence, band structures, density of states, and electron density difference.
- [48] Y. W. Li, B. Li, T. Cui, Y. Li, L. J. Zhang, Y. M. Ma, and G. T. Zou, *J. Phys. Condens. Matter* **20**, 045211 (2008).
- [49] Y. Li, Y. Ma, T. Cui, Y. Yan, and G. Zou, *Appl. Phys. Lett.* **92**, 101907 (2008).
- [50] Y. Li, Y. W. Li, Y. Ma, T. Cui, and G. Zou, *Phys. Rev. B* **81**, 052101 (2010).

- [51] J. Heyd, G. E. Scuseria, and M. Ernzerhof, *J. Chem. Phys.* **118**, 8207 (2003).
- [52] A. V. Krukau, O. A. Vydrov, A. F. Izmaylov, and G. E. Scuseria, *J. Chem. Phys.* **125**, 224106 (2006).
- [53] B. Rousseau, Y. Xie, Y. Ma, and A. Bergara, *Eur. Phys. J. B* **81**, 1 (2011).
- [54] A. Masago, K. Shirai, and H. Katayama-Yoshida, *Phys. Rev. B* **73**, 104102 (2006).
- [55] A. R. Oganov, J. Chen, C. Gatti, Y. Ma, C. W. Glass, Z. Liu, T. Yu, O. O. Kurakevych, and V. L. Solozhenko, *Nature (London)* **457**, 863 (2009).
- [56] W. Krätschmer, L. D. Lamb, K. Fostiropoulos, and D. R. Huffman, *Nature (London)* **347**, 354 (1990).
- [57] S. Yamanaka, E. Enishi, H. Fukuoka, and M. Yasukawa, *Inorg. Chem.* **39**, 56 (2000).
- [58] X. Wang, Y. Wang, M. Miao, X. Zhong, J. Lv, T. Cui, J. Li, L. Chen, C. J. Pickard, and Y. Ma, *Phys. Rev. Lett.* **109**, 175502 (2012).
- [59] W. B. Pearson, *Crystal Chemistry and Physics of Metals and Alloys* (Wiley, New York, 1972).